COBEM 2023 27TH INTERNATIONAL CONGRESS OF MECHANICAL ENGENEERING

ABCM Brazilian Society of Mechanical Sciences and Engineering
27th ABCM International Congress of Mechanical Engineering
December 04-08, 2023, Florianópolis-SC, Brazil

COB-2023-0660
STATIC STIFFNESS CORRELATION OF ELASTOMERIC BUSHINGS USING FINITE ELEMENT ANALYSIS

Luiz Felipe Sallani Simioni
Wallace Gusmão Ferreira
Universidade Federal do ABC - Av. dos Estados, 5001 – Bangu, Santo André - SP
luiz.simioni@aluno.ufabc.edu.br
wallace.ferreira@ufabc.edu.br

Fernando Santos
Ford Motor Company – Av. Dr. Cardoso de Melo, 1336 - Vila Olímpia, São Paulo - SP
fsanto59@ford.com

Abstract. The use of bushings in vehicle suspensions is a traditional way to reduce vibration, road noises and increase ride smoothness. However, the bushing design process relies heavily on experimental and historical data due to the complex nature of the elastomers used in it. The use of CAE software in this process is hindered by that complexity, given that the hyperelasticity present in elastomers can only be described using hyperelastic models such as Mooney-Rivlin, Ogden and Yeoh, which use a set of parameters to describe the elastomer's response. These parameters can be determined using curve fitting procedures that rely on test data, which is not always available and increases development costs. The traditional way to simulate a bushing consists of obtaining the geometry and material properties, modeling it in FEA software, applying boundary conditions and analyzing the results - This approach was executed during this work, however, during the research, a few obstacles were faced. For example, the elastomer constitutive behavior needs to be calibrated using experimental data given by its supplier, but this data is often difficult to obtain due to suppliers' limitations as well as physical limitations such as batch-to-batch rubber stiffness variability, where elastomers with the same Shore A hardness present different stiffnesses. These problems can be avoided by using an inverse analysis instead of the traditional direct method. The present work proposes a trust region dog-leg optimization routine that uses a MATLAB-ABAQUS interaction to find the hyperelastic parameters for a given geometry based on experimental data. The methodology was applied to example models such as 3D and axisymmetric models of automotive bushings using different types of data. It yielded results that showed a minimization of the discrepancy and, therefore, yielded parameters that could describe the constitutive behavior seen in the experimental or pseudo experimental data.

Keywords: *hyperelastic models, Optimization, bushing stiffness*

1. INTRODUCTION

Bushings are extensively used in the automotive industry due to their importance in noise and vibration reduction that can be achieved thanks to the presence of elastomers in the bushing structure. Elastomers, like the vulcanized rubber, are a highly complex material that differ from metals given that it cannot be represented using just a few mechanical properties like metals can (Lei et al., 2013) due to its hyperelastic nature. A hyperelastic material shows highly non-linear elastic isotropic behavior with incompressibility (Kaya et al., 2016).

Since classical mechanics theories like Hooke's Law cannot be applied to hyperelastic materials, several models have been developed throughout the years (Mooney, 1940; Twizell & Ogden, 1983; Yeoh, 1993) in search of a formulation that reliably characterizes the elastomer's mechanical behavior. Examples of these models include Neo-Hookean, Ogden, Yeoh, Arruda-Boyce and Mooney-Rivlin.

1.1 Hyperelastic Constitutive Models and Curve Fitting

Each model has a specific approach to modeling the material response based on its strain energy density function, which depends on the principal stretches or invariants of the strain tensor (D. Lalo & Greco, 2018). The hyperelastic models can then be classified as "I_1-based" or "Not I_1-based" depending on their formulation dependency on the first invariant. I_1-based models can be curve fitted using only one deformation mode meanwhile "Not I_1-based" needs experimental data from two or more deformation modes.

To use those constitutive laws, one must determine a set of coefficients, linear or non-linear, to fit a polynomial equation into a previously obtained set of test data, a process that is called curve fitting, as can be seen in Figure 1. This is the traditional way of characterizing hyperelastic models, especially in CAE software and can be done using software

such as Excel, MCalibration or ABAQUS/CAE, being the latter used in this work. However, it must be noted that this process has one major drawback: it depends on test data, which is not always available.

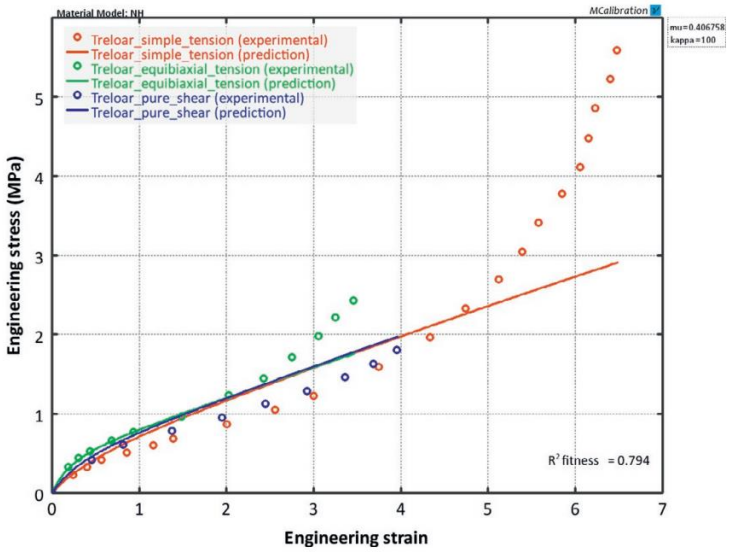

Figure 1. Comparison between experimental data points and predictions from a curve fitted Neo-Hookean model (Bergstrom, 2015)

1.2 Experimental data acquision

The experimental data is obtained through a series of tests that are performed using elastomeric specimens for data about the material such as uniaxial, biaxial, planar and volumetric deformation modes, as can be seen in Figure 2, that yield a stress-strain curve for each deformation mode. To use hyperelastic material models in a FE model, one must provide at least a uniaxial test data, however, a combination of one or more deformation mode tests results in a more accurate material model (Dassault Systems, 2021). Bushings can also be tested for the stiffness curves extraction in a range of modes: axial, radial, conical, and torsional, yielding a curve similar to the one seen in Figure 3.

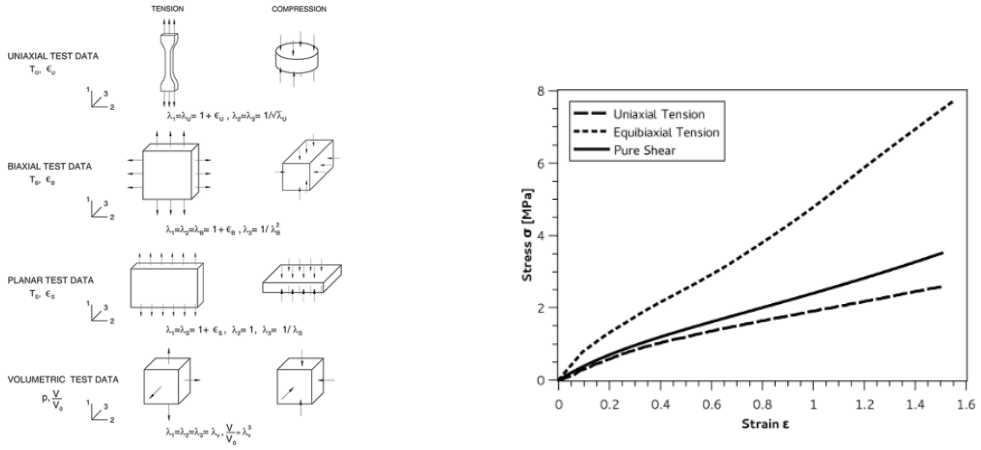

(a) (b)

Figure 2. (a) Deformation modes for specimen testing. (Dassault Systems, 2021) (b) Example of a stress-strain curve for a specimen test. (Javorik et al., 2018)

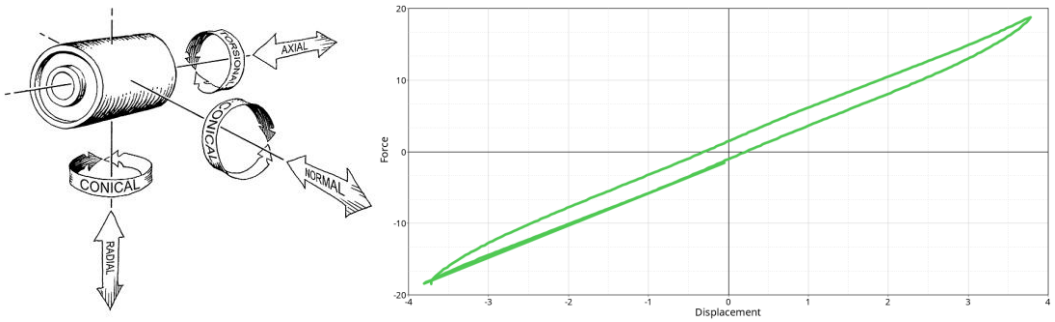

(a) (b)

Figure 3. (a) Deformation modes for bushing testing. (b) Example of a stiffness curve for an axial test

The difference between the loading and unloading curves in the force-displacement curve represents the phenomenon called “hysteresis” and the area between the curves represents energy being dissipated mainly as heat (D. F. Lalo, 2020). One other important phenomenon in bushing testing is the Mullins effect (Mullins, 1969), most evident during cyclic loading, which causes a progressive softening of the elastomer in each cycle, as Figure 4 shows. However, (Diani et al., 2009) says that the initial force-displacement curve obtained from the first loading step is unique and cannot be retraced, decreasing with each cycle until the response becomes stable.

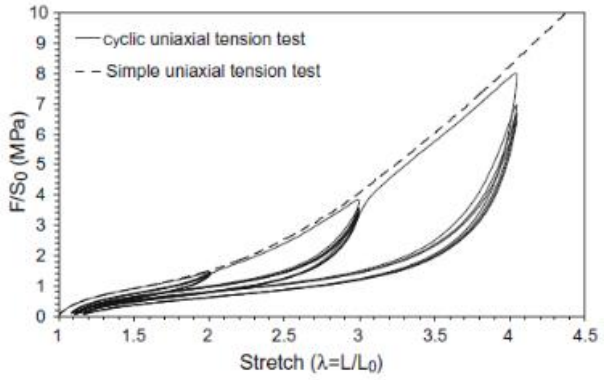

Figure 4: Stress-strain responses of a 50 phr carbon-black filled SBR submitted to a simple uniaxial tension and to a cyclic uniaxial tension with increasing maximum stretches every 5 cycles. Source: (Diani et al., 2009)

2. DIRECT METHOD

The direct method consists of the conventional way that a bushing is analyzed in CAE software, being a challenging task due to the elastomer’s complex hyperelastic behavior. The process, described in Figure 5, needs experimental data in two moments in order to correlate with the simulation: first, the experimental data from the elastomer so that the hyperelastic model can be curve fitted then experimental data from the bushing stiffness so that the CAE model can be correlated. After the analysis, the bushing stiffness curve can be extracted and compared to the experimental stiffness curve.

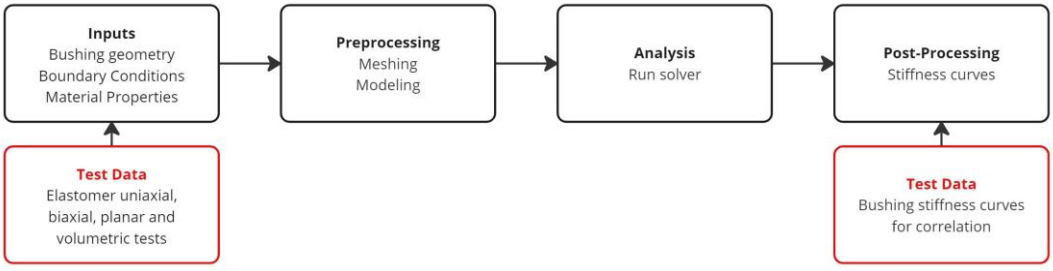

Figure 5. Direct Method flowchart

Using this approach, a finite element model of a bushing, composed of aluminum outer and inner rings and an elastomeric middle ring, was created using ABAQUS, as shown in Figure 6, aiming to simulate the test bench used to extract the experimental data.

The bushing was meshed using HEX8 elements throughout the whole model. However, in order to simulate a hyperelastic material, hybrid formulation HEX (C3D8H) elements were used in the elastomer while C3D8R elements were used in the inner and outer aluminum rings. The boundary conditions were applied accordingly, using a rigid element (KINCOUP-type element) in the center of the bushing for applying the loads in the axial (B1) and radial (B2) directions while the outer nodes of the outer ring were fixed in all six degrees of freedom (A). Given that the bushing can sustain heavy radial displacement, a self-contact was configured in the elastomer outer surfaces (D). For the interaction between the materials (C), a "glue"-type contact was applied. Due to the Mullins effect, the model was set up with six total load-unload cycles: five positive load-unload and one negative load-unload cycle.

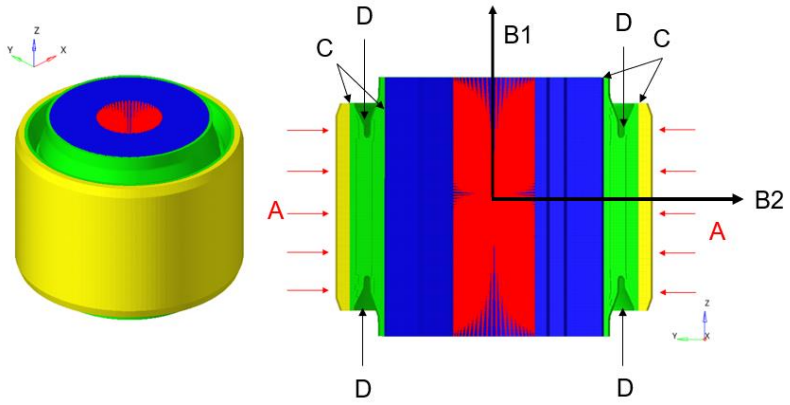

Figure 6: Bushing FE Model and Cross Section

The model was simulated using ABAQUS solver and its stiffness curves were extracted using the RBE3 independent node as the reference node for calculations. As seen in Figure 7, the results obtained were stiffer than the experimental curve – while the experimental bushing shows a stiffness of 363 N/mm, the FE model shows a stiffness of 645-655 N/mm, regardless of the material model used. After some research, it was found that the elastomers' mechanical properties vary significantly from batch to batch and therefore, one must guarantee that the elastomer used in the evaluated bushing is from the same batch as the elastomer evaluated in the first test. This was not the case with the model used in this work, which used different batches for the curve fitting procedure and the experimental curve.

The experimental data is usually given by the supplier, who does not guarantee that the elastomer evaluated for the uniaxial, biaxial, planar and volumetric tests is from the same batch that the elastomer used in the axial, radial and conical bushing tests. This poses a challenge for the correlation between CAE and experimental data, so another approach was needed.

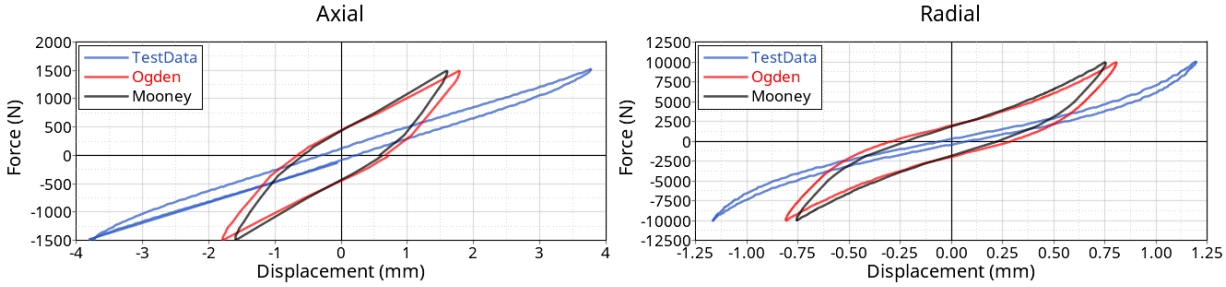

Figure 7: FE Model Stiffness curves vs. Experimental Stiffness Curves

3. INVERSE METHOD

Given that, for an accurate correlation, the direct method needs information that is not available, another approach must be used. In Figure 8, it can be seen that, in the direct method, one uses inputs (geometry, material properties, etc.) to find the output (stiffness curve) while in the inverse analysis, one uses the outputs to find the required inputs for that output – that is, in this work's context, with a stiffness curve, one can find the material properties that lead to that curve.

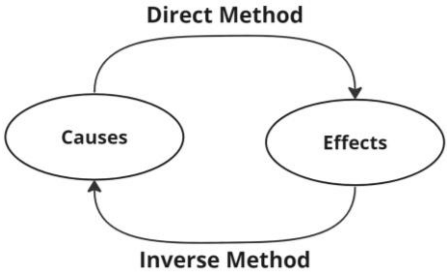

Figure 8: Scheme of solving direct/inverse problems. Adapted from (Buljak, 2012).

For this approach to work, one must guarantee that the model accurately represents the boundary conditions that were in place during testing, as well as eliminate any other source of error that could make the model not representative of the testing i.e., checking the inner and outer rings material properties and correctly modeling the contacts.

3.1 MATLAB-ABAQUS Algorithm

The algorithm was proposed by (Buljak, 2012) and adapted for this work's needs, as shown in Figure 9. It uses an ABAQUS-MATLAB interaction while running an optimization routine (which will be further detailed) that has the objective of minimizing the discrepancy between the experimental stiffness curve and the stiffness curve calculated by the algorithm.

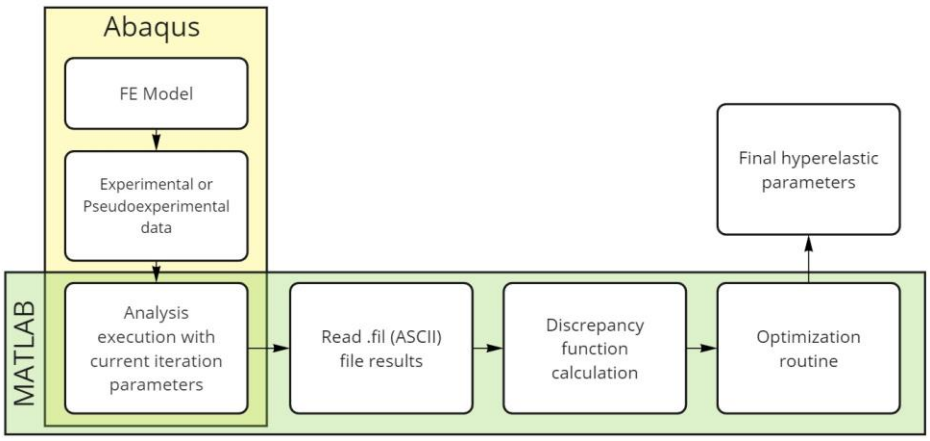

Figure 9. Flowchart of the MATLAB-ABAQUS algorithm.

The code starts by loading the experimental data into MATLAB, then it runs a simulation using the initial guess parameters provided by the user to calculate the discrepancy. After that, it uses another script to read the generated .fil file and extract the force-displacement information, creating the stiffness curve used in the discrepancy calculation. For that, it uses another script that takes the experimental and calculated stiffness curves and interpolates it in a normalized range, then the discrepancy is calculated, yielding the objective function value for the first iteration.

The optimization routine is then initiated, repeating this process, and changing the material parameters in the .inp file iteratively until the objective function is minimized and the optimal material parameters are found.

3.2 Optimization Routine

The optimization strategy used is a dogleg trust region with Cauchy point algorithm. It incorporates the advantages of each strategy such as the fast quadratic and global convergence provided by the dog-leg strategy as well as the computationally inexpensive function evaluation provided by the Cauchy point use (Buljak, 2012). Figure 10 shows the algorithm's architecture – it initiates by receiving the necessary input and configurations from the user, then it calculates the Hessian and gradient to check if the Hessian is positive-definite and if the gradient is not zero. Then, it calculates the Newton direction and uses it to define if the solution will be calculated via dogleg with Cauchy point or using the direction itself. After the objective function is calculated, the agreement ratio – a number that quantifies the model function and objective function agreement. If this ratio is greater than zero, it means that there's agreement, therefore, the step is accepted, and the parameters are updated and checked for convergence. If the ration is less than zero, it means there is a

significant disagreement and, therefore, the trust region must be reduced, and the step should be rejected so that another iteration might be tried. If this happens three times, the optimization is stopped since there was no improvement.

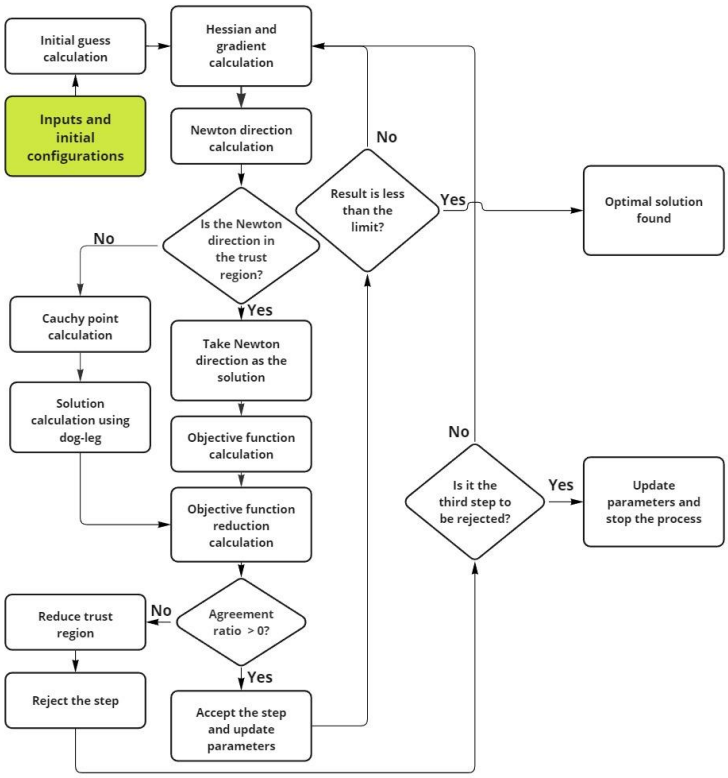

Figure 10: Dog-leg trust region optimization algorithm flowchart. Adapted from (Buljak, 2012).

4. RESULTS AND DISCUSSION

For this optimization routine, an axisymmetric model of the bushing was used in order to reduce computational costs, thus, only the axial load case could be simulated. Also, a Mooney-Rivlin hyperelastic model was used due to its simplicity – only two parameters are used. It is worth noting that it is generally accepted that a roughly 10% error between experimental and simulation results is acceptable for rubber materials (Kaya et al., 2016). Even so, the model did not converge into the acceptable range using experimental data. After some investigation, it was assumed that the Mooney-Rivlin model was too simple for the problem to converge and therefore, a more robust Yeoh model was used. However, as Figure 11 shows, the optimization did not converge within the acceptable range. Further tests were done but ended up with the same results.

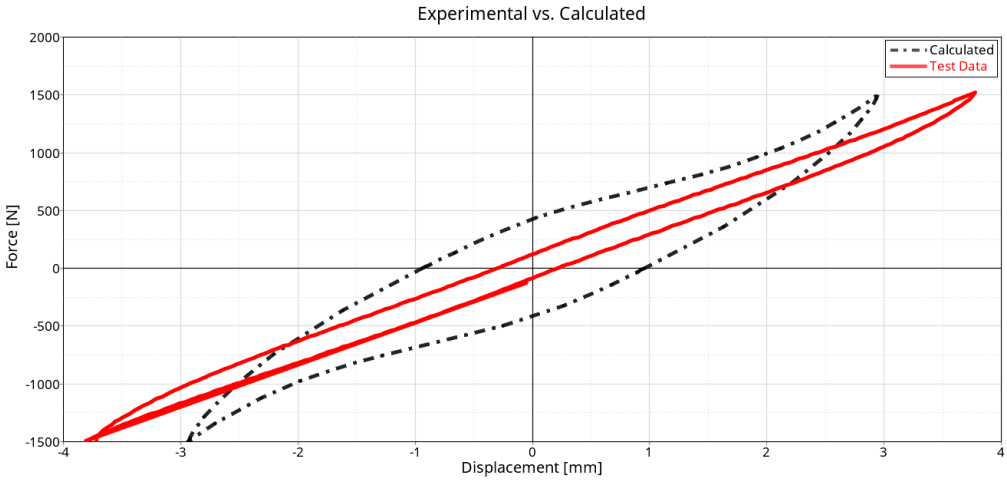

Figure 11: Yeoh model result

Since the model did not converge using experimental data, in order to verify if the model is capable of being solved, pseudo-experimental data was used. In other words, the experimental data used was extracted from a previous simulation where the hyperelastic material parameters are known. For this to work, one must be aware of the irrefutable inverse crime that, as defined by (Wirgin, 2004), "occurs when the same (or very nearly the same) theoretical ingredients are employed to synthesize as well as to invert data in an inverse problem". For the model used, this means that the mesh used to extract the pseudo-experimental data cannot be the same mesh as the one used in the calculations – in this work, a coarser mesh was used for data extraction, aiming to mimic real-world condition where data acquisition points are few.

Using this approach, more accurate results were obtained, as shown in Figure 12. The algorithm successfully yielded a set of material parameters that produced a curve similar to the pseudo-experimental one, but this set is different from the original set used for the data extraction. This shows two things: the algorithm can yield the parameters for the given model and the optimization problem is highly non-convex.

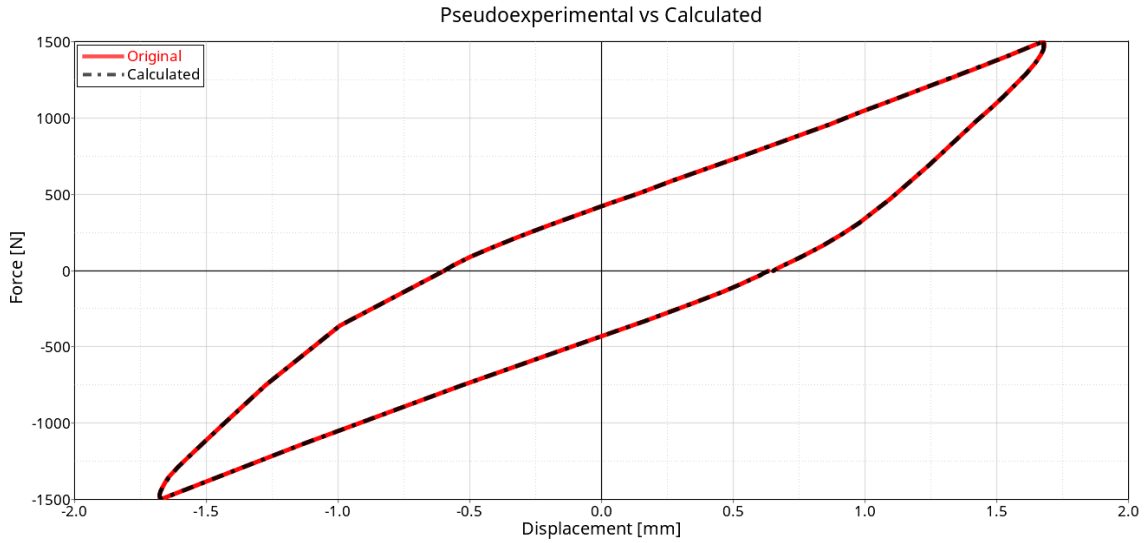

Figure 12: Pseudo-experimental model vs. Calculated model

The optimization routine is gradient-based and is subject to the limitation revolving around global and local minima. Given the non-convex nature of the problem, this poses a challenge: even if the routine uses several techniques to ensure a global convergence, it is subject to its own limitations, such as finding a local minimum and lack of bounds leading to infeasible sets of parameters and may not be the best approach to this kind of problem.

It is important to note that, with each iteration, no matter how many parameters there were - or their magnitude – the optimization routine changed all of them using an equal step. This, in addition to the lack of bounds for the parameters, led to the problem cited earlier: infeasible sets being used in the simulation, which, as expected, lead to errors. This optimization problem could potentially benefit from a more stochastic approach to optimization that a genetic algorithm offers, which can find the global minimum more efficiently.

5. CONCLUSION

In this work, a dog-leg trust region optimization routine was proposed in order to solve an inverse analysis problem which aimed to identify hyperelastic material parameters of an automotive bushing using experimental and pseudo-experimental data. By using an ABAQUS-MATLAB interaction script, the optimization routine could be executed in a simple and effective way. The proposed algorithm works for accurately predicting hyperelastic material parameters using inverse analysis based on pseudo-experimental data. However, when experimental data is used, the model does not converge to a solution, mostly due to the lack of bounds for the optimization problem, which leads to infeasible sets of parameters. For future works, this same optimization problem can be solved using a genetic algorithm, which could potentially increase its stability and accuracy.

6. ACKNOWLEDGEMENTS

We thank Ford Motor Company for providing all the necessary resources for this work to be executed. We also thank IEL – Instituto Euvaldo Lodi, which, through project CAE 21-03, provided resources for this work.

7. REFERENCES

Bergstrom, J. (2015). *Mechanics of Solid Polymers: Theory and Computational Modeling* (1st ed.).

Buljak, V. (2012). *Inverse Analyses with Model Reduction*. Springer Berlin Heidelberg. https://doi.org/10.1007/978-3-642-22703-5

Dassault Systems. (2021). *Abaqus Theory Manual* .

Diani, J., Fayolle, B., & Gilormini, P. (2009). A review on the Mullins effect. *European Polymer Journal*, *45*(3), 601–612. https://doi.org/10.1016/j.eurpolymj.2008.11.017

Javorik, J., Kledrowetz, J., Keerthiwansa, R., & Nekoksa, P. (2018). The numerical analysis of axially loaded elastomeric bushing. *Materials Science Forum*, *919*, 315–324. https://doi.org/10.4028/www.scientific.net/MSF.919.315

Kaya, N., Yavuz Erkek, M., & Güven, C. (2016). Hyperelastic modelling and shape optimisation of vehicle rubber bushings Hyperelastic modelling and shape optimisation of vehicle rubber bushings 213. In *Int. J. Vehicle Design* (Vol. 71).

Lalo, D. F. (2020). *Numerical modeling and experimental characterization of conical-laminated elastomeric bearings subjected to different modes of large multiaxial strains - An application of DIC technique in biaxial straining*. Universidade Federal de Minas Gerais.

Lalo, D., & Greco, M. (2018, February 15). *Rubber bushing hyperelastic behavior based on shore hardness and uniaxial extension*. https://doi.org/10.26678/abcm.cobem2017.cob17-5280

Lei, G., Chen, Q., Liu, Y., & Jiang, J. (2013). An inverse method to reconstruct complete stiffness information of rubber bushing. *Advances in Materials Science and Engineering*, *2013*. https://doi.org/10.1155/2013/187636

Mooney, M. (1940). A Theory of Large Elastic Deformation. *Journal of Applied Physics*, *11*(9), 582–592. https://doi.org/10.1063/1.1712836

Mullins, L. (1969). Softening of Rubber by Deformation. *Rubber Chemistry and Technology*, *42*(1), 339–362. https://doi.org/10.5254/1.3539210

Twizell, E. H., & Ogden, R. W. (1983). Non-linear optimization of the material constants in Ogden's stress-deformation function for incompressible isotropic elastic materials. *The Journal of the Australian Mathematical Society. Series B. Applied Mathematics*, *24*(4), 424–434. https://doi.org/10.1017/S0334270000003787

Wirgin, A. (2004). *The Inverse Crime*. https://arxiv.org/pdf/math-ph/0401050v1.pdf

Yeoh, O. H. (1993). Some Forms of the Strain Energy Function for Rubber. *Rubber Chemistry and Technology*, *66*(5), 754–771. https://doi.org/10.5254/1.3538343

8. RESPONSIBILITY NOTICE

The authors are the only ones responsible for the printed material included in this paper.